Direct imaging of fluorescent structures behind turbid layers

Giulia Ghielmetti[1] **and Christof M. Aegerter**[1,*]

[1]*Physik-Institut, University of Zurich, Winterthurerstrasse 190,*
8057 Zurich, Switzerland
[*]aegerter@physik.uzh.ch

Abstract: We present a method to directly image fluorescent structures inside turbid media. This is based on wave-front shaping to optimize the scattered light onto a single fluorescent particle, as the optical memory effect for a scanning image of the surroundings of this particle. We show that iterating the optimization leads to the focusing on a single particle whose surroundings are subsequently scanned. In combination with a parabolic phase pattern, this method can be extended to a three dimensional imaging method inside turbid media.

© 2014 Optical Society of America

OCIS codes: (290.4210) Multiple scattering; (110.0180) Microscopy; (110.7050) Turbid media; (030.6140) Speckle.

References and links

1. A. P. Mosk, A. Lagendijk, G. Lerosey, and M. Fink, "Controlling waves in space and time for imaging and focusing in complex media," Nat. Photonics **6**, 283–292 (2012).
2. I. M. Vellekoop and A. P. Mosk, "Focusing coherent light through opaque strongly scattering media," Opt. Lett. **32**, 2309–2311 (2007).
3. J. Aulbach, B. Gjonaj, P. M. Johnson, A. P. Mosk, and A. Lagendijk, "Control of light transmission through opaque scattering media in space and time," Phys. Rev. Lett. **106**, 103901 (2011).
4. O. Katz, E. Small, Y. Bromberg, and Y. Silberberg, "Focusing and compression of ultrashort pulses through scattering media," Nat. Photonics **5**, 372–377 (2011).
5. D. J. McCabe, A. Tajalli, D. R. Austin, P. Bondareff, I. A. Walmsley, S. Gigan, and B. Chatel, "Spatio-temporal focusing of an ultrafast pulse through a multiply scattering medium," Nat. Commun. **2**, 447 (2011).
6. J. H. Park, C. H. Park, H. Yu, Y. H. Cho, and Y. K. Park, "Active spectral filtering through turbid media," Opt. Lett. **37**, 3261–3263 (2012).
7. E. Small, O. Katz, Y. Guan, and Y. Silberberg, "Spectral control of broadband light through random media by wavefront shaping," Opt. Lett. **37**, 3429–3431 (2012).
8. J. H. Park, C. Park, H. Yu, Y. H. Cho, and Y. K. Park, "Dynamic active wave plate using random nanoparticles," Opt. Express **20**, 17010–17016 (2012).
9. Y. Guan, O. Katz, E. Small, J. Zhou, and Y. Silberberg, "Polarization control of multiply-scattered light through random media by wavefront shaping," Opt. Lett. **37**, 4463–4665 (2012).
10. R. Fiolka, K. Si, and M. Cui, "Complex wavefront corrections for deep tissue focusing using low coherence backscattered light," Opt. Express **20**, 16532–16543 (2012).
11. J. Jang, J. Lim, H. Yu, H. Choi, J. Ha, J. H. Park, W. Y. Oh, W. Jang, S. D. Lee, and Y. K. Park, "Complex wavefront shaping for optimal depth-selective focusing in optical coherence tomography," Opt. Express **21**, 2890–2902 (2013).
12. Y. Choi, T. R. Hillman, W. Choi, N. Lue, R. R. Dasari, P. T. So, W. Choi, and Z. Yaqoob, "Measurement of the time-resolved reflection matrix for enhancing light energy delivery into a scattering medium," Phys. Rev. Lett. **111**, 243901 (2013).
13. S. M. Popoff, G. Lerosey, M. Fink, A. C. Boccara, and S. Gigan, "Image transmission through an opaque material," Nat. Commun. **1**, 81 (2010).
14. I. M. Vellekoop and C. M. Aegerter, "Scattered light fluorescence microscopy: imaging through turbid layers," Opt. Lett. **35**, 1245–1247 (2010).

15. G. Ghielmetti and C. M. Aegerter, "Scattered light fluorescence microscopy in three dimensions," Opt. Lett. **20**, 3744–3752 (2012).
16. C. L. Hsieh, Y. Pu, R. Grange, G. Laporte, and D. Psaltis, "Imaging through turbid layers by scanning the phase conjugated second harmonic radiation from a nanoparticle," Opt. Express **18**, 20723–20731 (2010).
17. X. Yang, C. L. Hsieh, Y. Pu, and D. Psaltis, "Three-dimensional scanning microscopy through thin turbid media," Opt. Express **20**, 2500–2506 (2012).
18. J. Bertolotti, E. G. van Putten, C. Blum, A. Lagendijk, W. L. Vos, and A. P. Mosk, "Non-invasive imaging through opaque scattering layers," Nature **491**, 232–234 (2012).
19. D. B. Conkey, A. M. Caravaca-Aguirre, and R. Piestun, "High-speed scattering medium characterization with application to focusing light through turbid media," Opt. Express **20**, 1733–1740 (2012).
20. I. Freund, M. Rosenbluh, and S. Feng, "Memory effects in propagation of optical waves through disordered media," Phys. Rev. Lett. **61**, 2328–2331 (1988).
21. D. L. Fried, "Anisoplanatism in adaptive optics," J. Opt. Soc. Am. **72**, 52–61 (1982).
22. S. Feng, C. Kane, P. A. Lee, and A. D. Stone, "Correlations and fluctuations of coherent wave transmission through disordered media," Phys. Rev. Lett. **61**, 834–837 (1988).
23. Z. Yaqoob, D. Psaltis, M. S. Feld, and C. Yang, "Optical phase conjugation for turbidity suppression in biological samples," Nat. Photonics **2**, 110–115 (2008).
24. S. M. Popoff, G. Lerosey, R. Carminati, M. Fink, A. C. Boccara, and S. Gigan, "Measuring the transmission matrix in optics: an approach to the study and control of light propagation in disordered media," Phys. Rev. Lett. **104**, 100601 (2010).
25. S. M. Popoff, A. Aubry, G. Lerosey, M. Fink, A. C. Boccara, and S. Gigan, "Exploiting the time-reversal operator for adaptive optics, selective focusing, and scattering pattern analysis," Phys. Rev. Lett. **107**, 263901 (2011).
26. C. Prada and M. Fink, "Eigenmodes of the time reversal operator: A solution to selective focusing in multiple-target media," Wave Motion **20**, 151–163 (1994).
27. I. M. Vellekoop, E. G. van Putten, A. Lagendijk, and A. P. Mosk, "Demixing light paths inside disordered meta-materials," Opt. Express **16**, 67–80 (2008).
28. D. Akbulut, T. J. Huisman, E. G. van Putten, W. L. Vos, and A. P. Mosk, "Focusing light through random photonic media by binary amplitude modulation," Opt. Express **19**, 4017–4029 (2011).
29. D. B. Conkey, A. M. Caravaca-Aguirre, and R. Piestun, "High-speed scattering medium characterization with application to focusing light through turbid media," Opt. Express **20**, 1733–1740 (2012).
30. M. Cui, "A high speed wavefront determination method based on spatial frequency modulations for focusing light through random scattering media," Opt. Express **19**, 2989–2995 (2011).
31. I. M. Vellekoop and C. M. Aegerter, "Focusing light through living tissue," Proc. SPIE **7554**, 755430 (2010).

---

1. Introduction

With the advent of wave-front shaping in extremely turbid media allowing the control of diffusely scattered light [1] either in transmission [2, 3, 4, 5, 6, 7, 8, 9] or in reflection [10, 11, 12], imaging behind or inside turbid media has found renewed interest [13, 14, 15, 16, 17, 18, 19]. There have been several methods proposed, which all rely on the memory effect of multiply scattered light in order to scan the diffuse light behind a layer of turbid material [20, 21, 22]. Initial proposals have created a focus behind the turbid layer, either using direct optical access and wave-front shaping [2] or phase conjugation using second harmonic particles [23], which was then scanned for obtaining an image [14, 16]. Both of these methods are however invasive in that they need either some form of optical access for the wave-front optimization or the preparation of second harmonic particles in the sample. Subsequently, the determination of the transmission matrix [24] has been used to transport images through turbid layers [13], however also here optical access needed to be present. This has been extended recently to focus on structures without direct access by the determination of the singluar values of the transmission matrix, which gives access to the diminishingly brighter structures hidden behind the turbid layer [25]. Finally, a computational method based on the memory effect was presented recently, where the wave-front is not adjusted, but the speckle pattern is scanned across a fluorescent structure and the inverse problem is solved to obtain the structure behind the turbid medium [18]. The solution is however not necessarily unique and additional assumptions on the image need to be made in order to find an image.

In order to overcome the limitation of the necessity of optical access to a direct imaging

of fluorescent structures using wave-front shaping, it has been proposed to use the signal of a fluorescent particle for the optimization algorithm and subsequent formation of a focus [14, 27]. This focus would then be scanned to obtain an image of fluorescent structures in the vicinity. The challenge for this proposed technique is that it has only been demonstrated that the solution is unique for a single fluorescent particle. Therefore, one would either need to have a single focusing particle in a structure of different fluorescent particles, albeit with the same absorption properties, or one would have to find a method with which to ensure that even in the presence of several fluorescent particles, only one would have to be used for the focus and the subsequent imaging. In the present paper we will follow this second route and show that an iteration of the optimization algorithm on the fluorescence signal can be used to focus on the brightest particle, whose surrounding can then be scanned using the optical memory effect [14, 15]. This iterative technique is based on previous experiments in acoustic waves, where the focusing on scattering structures has been demonstrated as well [26]. Similarly, the method of the transmission matrix described above has similar features [25], where the different iterations in our case correspond to the different singular Eigenvalues of the transmission matrix and thus the different fluorescent particles.

We will describe the setup and the samples used in the next section, where fluorescent nanoparticles are used for imaging, which are hidden behind a turbid screen. Using the transmitted fluorescent intensity, we shape the incoming wave-front in order to focus the intensity on one or several fluorescent particles. We will show, that this optimization will lead to the focusing on a single particle after only a few iterations, even in the presence of many fluorescent particles. Once such a focus is found, the focus is scanned around the region of interest and a diffraction limited image of the fluorescent structures in the neighborhood is obtained. We conclude by putting the method in context and describing further extensions in order to create a three dimensional scanning microscope in turbid media.

2. Setup and samples

The sample consists in a 2mm thick glass-plate with a diffusing 1500 grit polished side 6 μm thick, corresponding to a few mean free paths. On the back, fluorescent nanobeads of 450 nm diameter are applied. The maximum of the excitation spectrum is at 480 nm, while the maximum of the emission is at 530 nm.

A schematic representation of the optical setup is shown in Fig. 1. A laser beam of 488 nm wavelength (Spectra- Physics Cyan 40 mW, 488 nm) passes through a galvo-scanner (General Scanning LDS-07-OH), which allows to move the beam in the $x - y$ plane. This beam is spatially expanded and sent to the SLM (Holoeye HEO 1080 P), which allows to perform the optimization to create the focus. The light on the SLM is imaged onto the sample through a 40x microscope objective (Zeiss A-Plan 40x/0.25) which creates a spot of a diameter of 80 μm on the turbid layer. After passing through the sample, the light goes through a Semrock filter (GFP-3035B) to block the illuminating blue laser light, and is collected by a camera (AVT Stingray F-145B) detecting the fluorescent signal.

3. Principle

To create the focus we optimize the phase of the different segments of the SLM in such a way that the integrated fluorescent intensity on the camera is maximized. Thus even in the absence of optical access, there is a contrast mechanism, which can be used to guide the wave-front optimization, since the maximization of the fluorescent intensity corresponds to an enhanced illumination of the fluorescent particle. In the presence of a single fluorescent particle, as was the case in [27], this directly means that we are creating a focus on that bead.
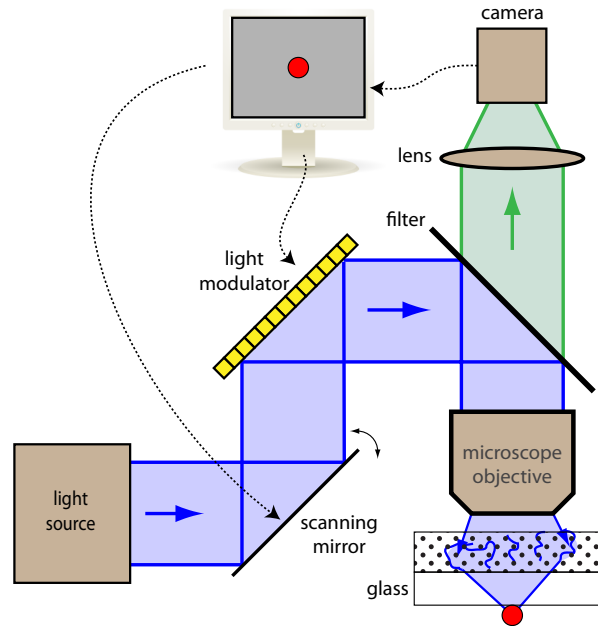
Fig. 1. Schematic setup of the experiment. The expanded laser beam goes through a galvo-scanner which allows to move the focus on a $x-y$ plane. It then goes on the SLM, and is imaged on the surface of the sample. The fluorescent light is collected by a camera located behind a fluorescence filter. The sample is a 2mm thick glass, with a diffusing 1500 grit polished side. On the back of the glass, there are fluorescent latex beads of 450 nm diameter.

The optimization algorithm works on segments, i.e. blocks of pixels, defined over the surface of the SLM. Each segment is processed by the following three steps. First, the algorithm measures the intensity of the fluorescence for five gray scale values applied to all the pixels of the current SLM segment. Second, it fits the five measured intensities with a sinus and third, it chooses the gray scale value corresponding to the maximum of the sinus for the segment. The intensity enhancement of the focus depends on the number of segments [2]. Since the fluorescence signal is low compared to the background, we need to start with large segments to increase the signal. The algorithm can be reiterated with smaller segments until the desired intensity magnification is reached.

Notice that, this algorithm does not have a notion of the source of the fluorescence. More specifically, in the case of multiple fluorescent beads, the algorithm does not know about them. The optimization will only consider the overall intensity, and optimize for it. This means that there are several local minima, which can be arrived at by an optimization. Therefore in the presence of several fluorescent sources a single optimization will not necessarily give a focus on a single bead. However, when iterating the optimization, a process akin to that observed in acoustic waves can be followed. Given the different starting conditions, where some fluorescent sources are strongly illuminated, the optimization will lead to a stronger illumination of the already selected sources leading to a successive enhancement of the strongest source. This process is strongly enhanced by a non-linear response of the fluorescent particles to the illumination. We refer to this with the notion of 'selection'.

Once a single fluorescent particle is illuminated, we have a focus, which can then be scanned by tilting the incoming beam through the galvo-scanner. This tilt corresponds to the addition of

a linear phase to the beam, which due to the memory effect is conserved behind the turbid layer and thus leads to a shift of the focus in the $x-y$ plane [14]. Capturing the integrated fluorescence of the scanned beam can then be used to obtain a fluorescence image of the neighborhood of the selected particle.
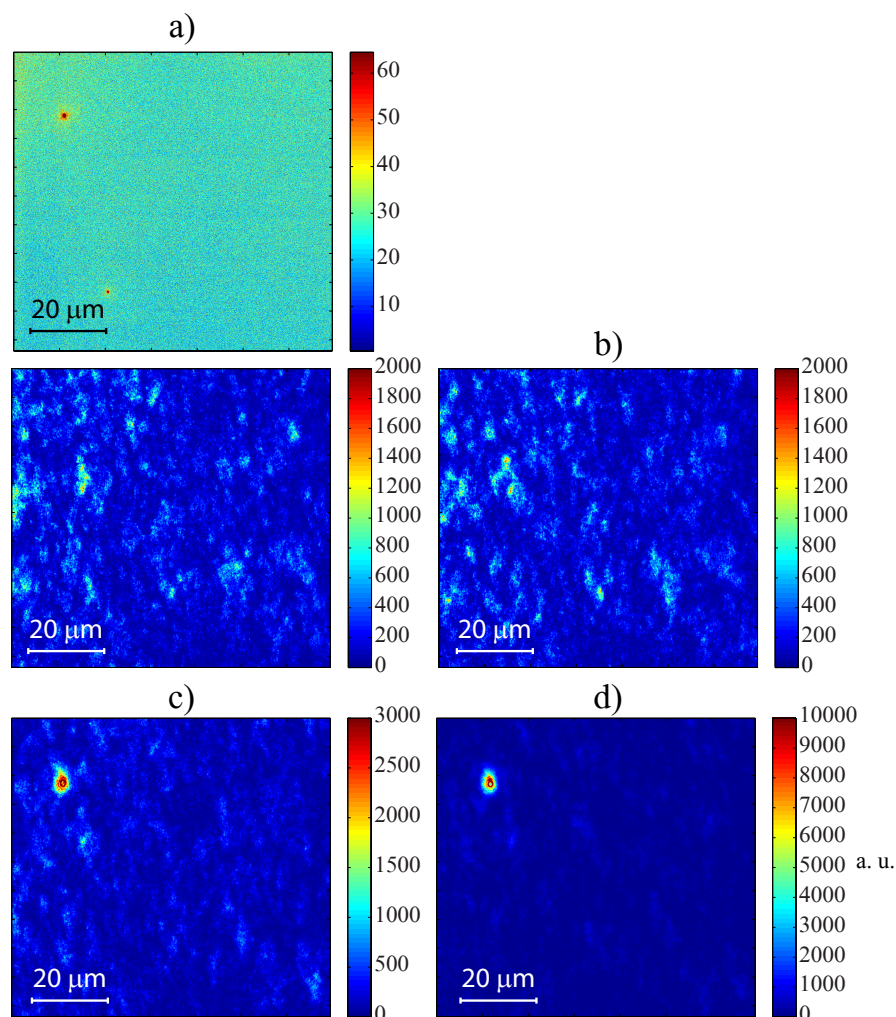
4. Experimental results

Fig. 2. Panels a) show a direct image of the fluorescent structures behind the turbid layer, consisting of two 450nm big fluorescent beads, and the transmitted light at the initial state. Panels b) through d) show the transmitted light distribution after successive iterations with 7x7 (b), 14x14 (c) and 28x28 (d) segments on the SLM. The intensity of the focus increases with the number of segments, while the fluorescence intensity decreases eventually due to photobleaching.

In Fig. 2 we show a focus created on a 450 nm diameter fluorescent bead behind a turbid layer after three iterations of the optimization algorithm, with different number of segments on the SLM: 7x7, 14x14 and 28x28. The fluorescence image of the initial situation shows two beads.

The optimization process selects the most emitting one, i.e. it results in the most emitting one being focused on. As said above, the intensity of the focus depends on the number of segments on the SLM [2]. With 28x28 segments we obtain an amplification of the intensity of about 200 times. The first iterations are needed to increase the signal with respect to the background, otherwise the contribution of the small segments can not be detected.

The focus shows a pattern coming from diffraction effects, since the dimension of the bead is of the order of the wavelength.

If there are more beads emitting similar intensity on the sample the system can initially create several foci. As noted above, iteration of the optimization leads to a choice of a different local maximum, such that, after some iterations, a single focus is obtained. This is shown in Fig. 3, where the iteration procedure is shown for a situation where several particles of comparable intensity are in the field of view, but we are still left with a single focus after a round of four iterations. In this case, the illumination time after an iteration was very long, such that the initially enhanced bead showed photo-bleaching in successive iterations. However in these iterations the next brightest bead is selected. Note also that in Fig. 3, the number of optimized segments is small, such that bright speckle spots are only weakly suppressed by the focus. A case with even more fluorescent sources is shown in Fig. 4. As can be seen in the sequence of iterations, the selection of a fluorescent bead depends on the brightness of the initial speckle illumination as well as the inherent brightness of the fluorescent beads. This shows that, even starting from complicated fluorescent structures, it is always possible to get a focus.

The quality of the focus and the possibility to image complex structures in this way is shown in Fig. 5. Here, several fluorescent particles are present in the field of view, where focusing has been performed to select one of them (noted with an arrow). This focus, is then scanned using the memory effect [20] in the vicinity of the particle, allowing to reconstruct the fluorescent structure. In this case, the scanning is done in the $x - y$ plane, perpendicular to the beam, at the depth of the focus. According to our previous work [15], a scanning in three dimensions would however also be possible.

5. Conclusion

In conclusion, we have shown a method with which to directly image fluorescent structures inside turbid media at diffraction limited resolution, in a non-invasive way. The basis of this technique are iterative wave-front shaping on the transmitted fluorescence, which selects a single particle creating a scannable focus. Since the focal sport size created using wave-front shaping is independent of the thickness of the turbid layer, a diffraction limited resolution can be achieved irrespective of the thickness of the turbid layer. The scanning is possible due to the optical memory effect and can be extended to three dimensions by the addition of a parabolic phase field to the SLM [15]. The scannable range is therefore limited by the optical thickness of the turbid layer [14], but in our case is at least a window of $15 \times 15 \mu m^2$. Due to the speed of the SLM, the imaging time is rather long, taking several minutes per iteration, such that applications can for the moment only be envisaged in static turbid media, i.e. where the turbid layer is stable on time-scales longer than the focusing time. However, using faster SLM's based on piezoelectric mirrors [28, 29], much faster focusing can in principle be achieved making application in biological systems possible [30, 31].
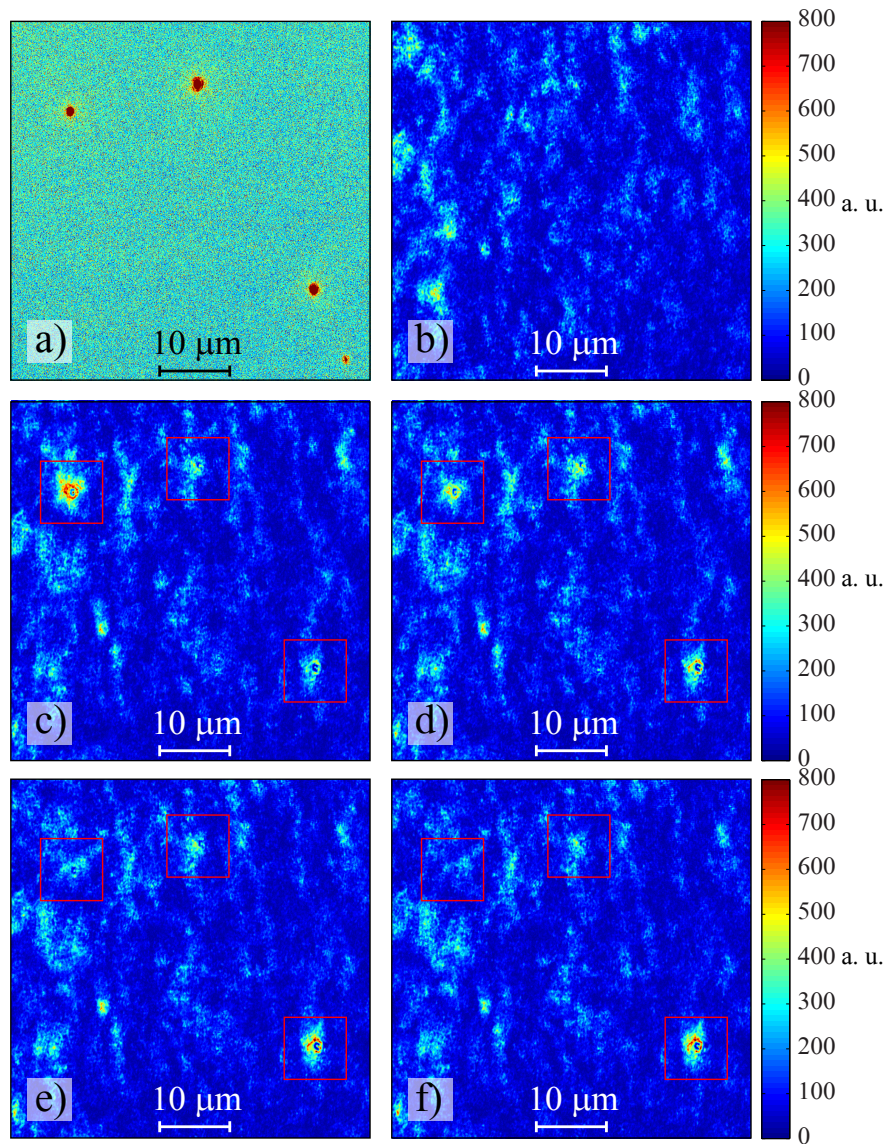
Fig. 3. The topleft panel (a) again shows the direct image of a set of four fluorescent particles (450 nm in diameter) hidden behind a turbid screen. Panel b) shows the transmitted light at the initial state. Panels c) through f) show the transmitted light after successive iterations with 14x14 segments controlled on the SLM. The red squares indicates the positions of the beads. After the fourth iteration with 14x14 segments the system selects one bead and a single focus is left.
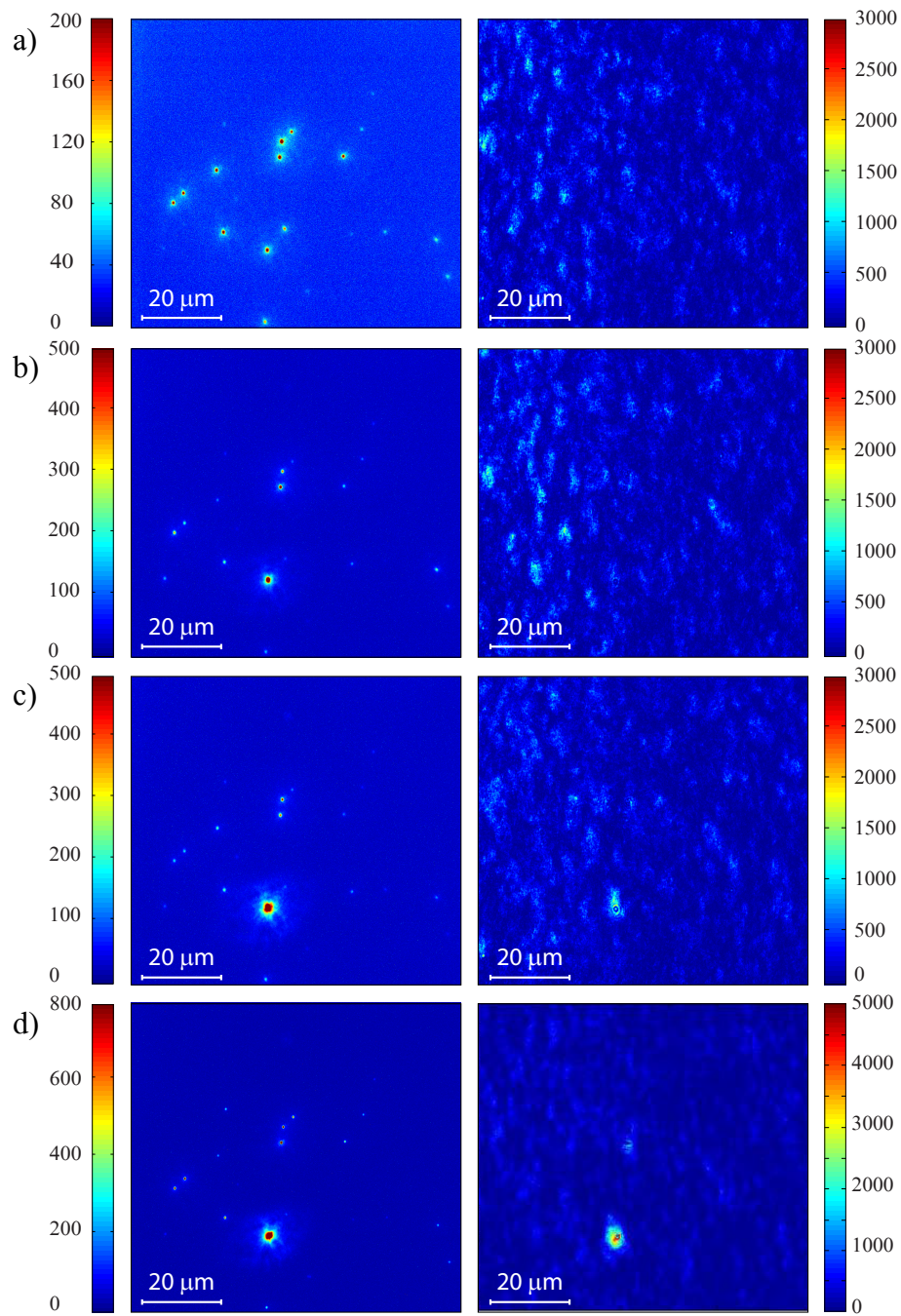
Fig. 4. In the presence of a large number of beads, the iterative scheme still works. a) show a field of view with more than 10 fluorescent sources ant the transmitted light. Panels b) to c) show the field of view (first column) and the transmitted light (second column) after iterations with 7x7 (b), 14x14 (c) and 28x28 (d) segments. At the end there is only a focus on a single fluorescent particle.
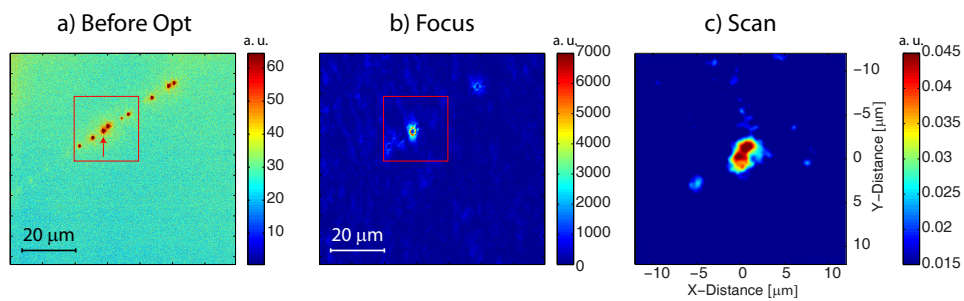
Fig. 5. a) shows the fluorescent beads on the sample, b) shows the focus obtained with 30x30 segments on the SLM and c) shows the result of the scanning. The red squares show the scanning area. The beads which are not in the center of the image are more difficult to detect because of two reasons: they have to be exactly on the $x-y$ plane to be detected, and the intensity of the focus decreases the more it is far away from the center.